Dhaka Univ. J. Sci. 58(2): 151-156, 2010 (July)

Designing Imbricated Cells Multilevel PWM Inverter for Large Induction Motor Drive

Sazzad Muhammad Samaun Imran, Rezaul Karim Mazumder and Subrata Kumar Aditya

Department of Applied Physics, Electronics & Communication Engineering, Dhaka University, Dhaka-1000, Bangladesh

Received on 25.09.2008. Accepted for Publication on 04.02.2010.

Abstract

Multilevel inverters have been attracting attention in recent years due to high power quality, high-voltage capability, low switching losses, and low EMC concerns. Hence a detailed work has been done on the design and performance study of a three-phase five-level imbricated cells PWM inverter. The heavy and bulky transformers that have been used in traditional inverters are eliminated completely from the system. Sine-triangle pulse width modulation technique has been used to generate the switching signal of the inverter. The designed inverter is targeted for loads that require high VA rating such as induction motor in industries. An LC filter has been used to minimize the harmonic distortion at a tolerable value. The designed inverter has been tested on a three-phase induction motor and found voltage, current and speed characteristics satisfactory.

Keywords: Multilevel inverter, Pulse width modulation, Induction motor, Total harmonic distortion, Imbricated cells inverter.

I. Introduction

Power electronic inverters are widely used in industrial power conversion systems both for utility and drives applications. A multilevel inverter can be implemented in many different ways, each with attendant advantages and disadvantages. Pulse-width modulation (PWM) of multi-level inverters is typically an extension of two-level methods. The most common types of multi-level voltage-source PWM are sine-triangle modulation and space vector modulation (SVM). The main function of a multilevel inverter is to produce a desired ac voltage waveform from several levels of dc voltages. These dc voltages may or may not be equal to one another. The staircase waveform produced by the multilevel inverter contains sharp transitions and results harmonics. The harmonics generated on the AC side greatly influence the power quality of the control system. The multi-level inverter improves the AC power quality by performing the power conversion in small voltage steps leading to lower harmonics. One of the significant advantages of multilevel configuration is the harmonic reduction in the output waveform without increasing switching frequency or decreasing the inverter power output [1], [2], [3].

II. Five-Level Imbricated Cells Inverter

Probably the most important multilevel topology to appear recently is the flying capacitor inverter, or imbricated cells multilevel inverter, proposed by Meynard and Foch [4], [5], [6]. Fig. 1 shows the structure for the a-phase of the five-level imbricated cell inverter.

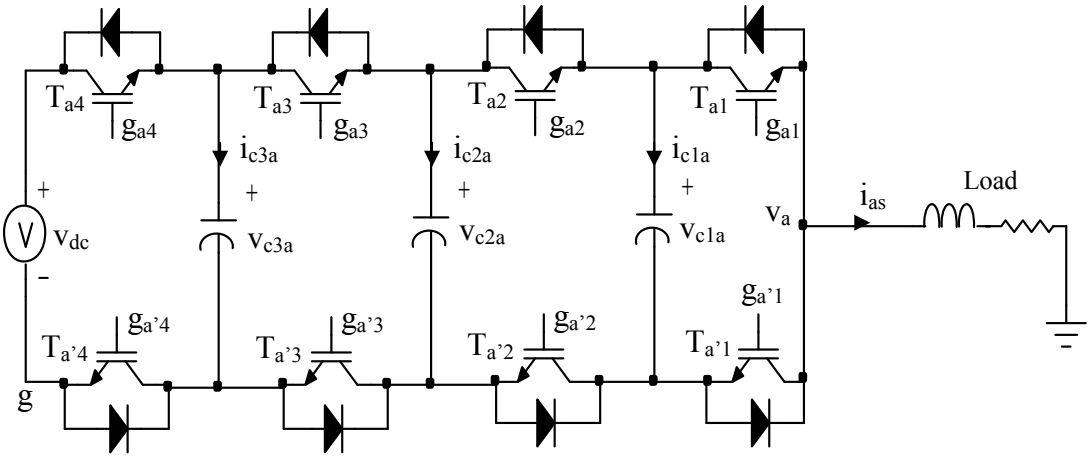

Fig. 1. Four-cell FCMI inverter topology (single-phase)

For this inverter, each capacitor is charged to a different voltage levels and the voltages of capacitors must be:

$$v_{c1a} = \frac{3}{4}v_{dc},\ v_{c2a} = \frac{2}{4}v_{dc},\ v_{c3a} = \frac{1}{4}v_{dc} \tag{1}$$

And if the required rms voltage is V_{rms}, then the input dc voltage must be

$$v_{dc} = V_p = V_{rms} \times \sqrt{2} \tag{2}$$

For the analysis presented herein, the line-to-ground voltage and capacitor currents can be expressed as,

$$\begin{aligned} v_{ag} &= (T_{a4})v_{dc} + (T_{a3} - T_{a4})v_{c3a} + \\ &\quad (T_{a2} - T_{a3})v_{c2a} + (T_{a1} - T_{a2})v_{c1a} \end{aligned} \tag{3}$$

$$\begin{aligned} i_{c1a} &= (T_{a2} - T_{a1})i_{as}, \\ i_{c2a} &= (T_{a3} - T_{a2})i_{as}, \\ i_{c3a} &= (T_{a4} - T_{a3})i_{as} \end{aligned} \tag{4}$$

Based on these fundamental equations, the line-to-ground voltage and capacitor currents can be determined for all combinations of transistor signals. The combination of

conducting switches and capacitors ensures that the voltage across any blocking switch is always well defined. Table 1 below shows the various switch combination of the voltage levels and their corresponding switch states.

Table 1: Switch combination of the voltage levels and their corresponding switch states

Output V_{AO}	S_1	S_2	S_3	S_4	S_5	S_6	S_7	S_8
$V_5=V_{dc}$	1	1	1	1	0	0	0	0
$V_4=3V_{dc}/4$	1	1	1	0	0	0	0	1
	1	1	0	1	0	0	1	0
	1	0	1	1	0	1	0	0
	0	1	1	1	1	0	0	0
$V_3=V_{dc}/2$	1	1	0	0	0	0	1	1
	1	0	1	0	0	1	0	1
	1	0	0	1	0	1	1	0
	0	1	1	0	1	0	0	1
	0	1	0	1	1	0	1	0
	0	0	1	1	1	1	0	0
$V_2=V_{dc}/4$	1	0	0	0	0	1	1	1
	0	1	0	0	1	0	1	1
	0	0	1	0	1	1	0	1
	0	0	0	1	1	1	1	0
$V_1=0$	0	0	0	0	1	1	1	1

For practical implementation, the switching state needs to be converted into transistor signals. Considering Table 1 this can be accomplished in general by,

$$T_{ai} = \begin{cases} 1 & s_a \geq i \\ 0 & elsewhere \end{cases} \quad (5)$$

An inverse relationship may also be useful and is given by,

$$s_a = \sum_{i=1}^{n-1} T_{ai} \quad (6)$$

Once the transistor signals are established, general expressions for the a-phase line-to-ground voltage and the a-phase component of the dc currents can be written as,

$$v_{ag} = \sum_{i=1}^{n-1} T_{ai} v_{cia} \quad (7)$$

$$i_{dcia} = [T_{a(i+1)} - T_{ai}] i_{as} \quad \text{for i=1,2,…,(n-2)} \quad (8)$$

For the general n-level imbricated cell inverter, the transistor voltages can be determined from the transistor signals by,

$$v_{Tai} = (1 - T_{ai})[v_{cia} - v_{c(i-1)a} - I_a v_{sw} + (1 - I_a) v_d] + T_{ai}[I_a v_{sw} - (1 - I_a) v_d] \quad (9)$$

where v_{sw} and v_d are the transistor and diode on-state voltage drops respectively and I_a is a logic flag representing the direction of the a-phase current.

$$I_a = \begin{cases} 1 & i_{as} \rangle 0 \\ 0 & elsewhere \end{cases} \quad (10)$$

When employing equation (9), the lowest and highest capacitor voltages will be $Vcoa^{=0}$ and $Vc(n-1)a^{=Vdc}$. The transistor and diode currents can be calculated using the following equations.

$$i_{T_{ai}} = T_{ai} I_a i_{as}, \; i_{DT_{ai}} = T_{ai}(1 - I_a) i_{as} \quad (11)$$

The capacitor currents can be calculated based on KCL equations as,

$$i_{cia} = i_{T_{a(i+1)}} - i_{T_{ai}} \quad (12)$$

The three-phase implementation of multi-level inverter involves three branches of the structure shown in Fig. 1 connected in parallel on the dc side and connected to wye-configured load on the ac side.

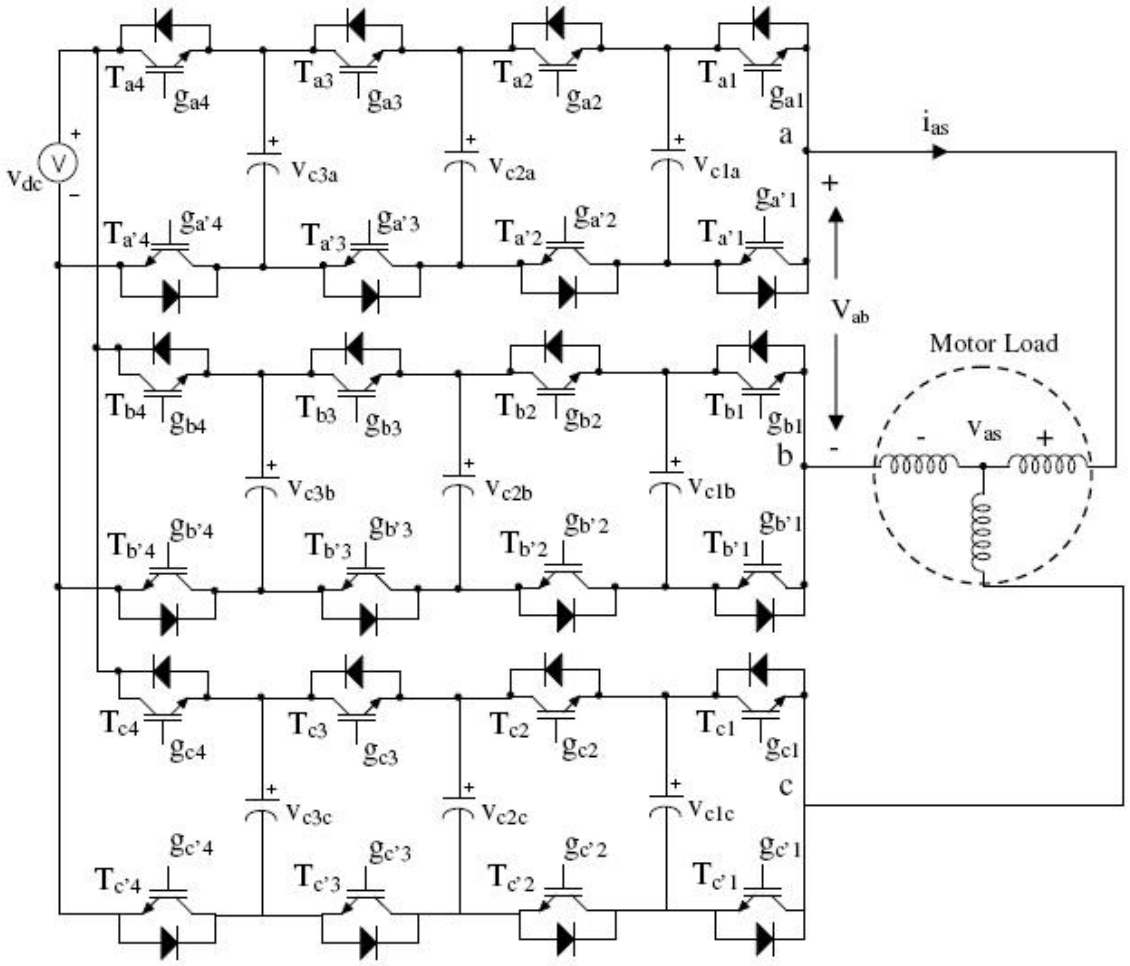

Fig. 2. Three-phase five-level imbricated cell inverter structure

Assuming proper operation, the inverter output line-to-ground voltages follow the switching states as,

$$\begin{bmatrix} v_{ag} \\ v_{bg} \\ v_{cg} \end{bmatrix} = \left(\frac{v_{dc}}{n-1}\right)\begin{bmatrix} s_a \\ s_b \\ s_c \end{bmatrix} \tag{13}$$

The line-to-neutral voltages may be determined directly from the line-to-ground voltages by [7],

$$\begin{bmatrix} v_{an} \\ v_{bn} \\ v_{cn} \end{bmatrix} = \frac{1}{3}\begin{bmatrix} 2 & -1 & -1 \\ -1 & 2 & -1 \\ -1 & -1 & 2 \end{bmatrix}\begin{bmatrix} v_{ag} \\ v_{bg} \\ v_{cg} \end{bmatrix} \tag{14}$$

Inverter line-to-line voltages are related to the line-to-ground voltages by,

$$\begin{bmatrix} v_{ab} \\ v_{bc} \\ v_{ca} \end{bmatrix} = \begin{bmatrix} 1 & -1 & 0 \\ 0 & 1 & -1 \\ -1 & 0 & 1 \end{bmatrix}\begin{bmatrix} v_{ag} \\ v_{bg} \\ v_{cg} \end{bmatrix} \tag{15}$$

Fig. 3 and Fig. 4 below show the line-to-ground voltage, and line-to-line voltage respectively for five-level inverter (n=5).

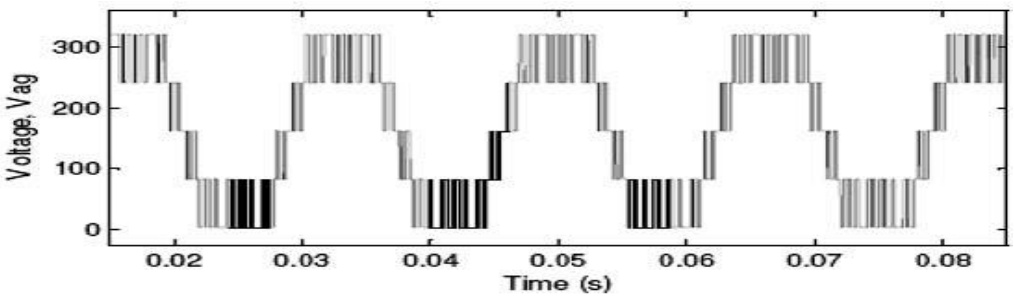

Fig. 3. Five-level inverter line-to-ground voltage waveform

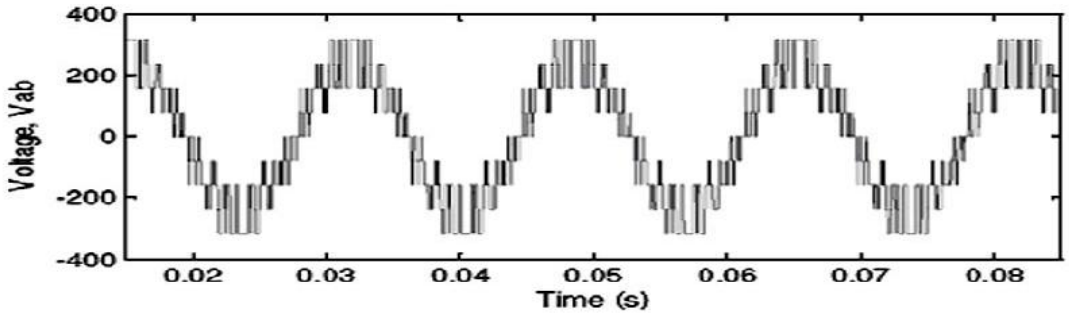

Fig. 4. Five-level inverter line-to-line voltage waveform

III. Sine-Triangle Pulse Width Modulator

The basis of the modulation method used herein is to define duty-cycles (modulating signals) for each phase, which will be based on commanded line-to-ground voltages [8]. The duty cycles are,

$$\begin{bmatrix} d_{am} \\ d_{bm} \\ d_{cm} \end{bmatrix} = \begin{bmatrix} m\cos(\theta_c) \\ m\cos(\theta_c - \frac{2\pi}{3}) \\ m\cos(\theta_c + \frac{2\pi}{3}) \end{bmatrix} + \left[1 - \frac{m}{6}\cos(3\theta_c)\right]\begin{bmatrix} 1 \\ 1 \\ 1 \end{bmatrix} \quad (16)$$

where $\theta_c=\omega_c t$ is the inverter electrical angle

and m is the modulation index which has a range of

$$0 \le m \le \frac{2}{\sqrt{3}} \quad (17)$$

The triangular carrier signals used in this work are given by,

$$c_i(t) = 1 + \frac{2}{\pi}(a\sin(\sin(N\theta_c - \phi_i))) \quad (18)$$

where $N = \frac{f_{car}}{f_{con}}$ = frequency modulation ratio

ϕ_i = phase of the carrier

f_{car} = carrier frequency

f_{con} = control frequency

For five-level three-phase systems, three control signals of different phase angles are needed. These three control signals of phase difference of 120^0 with each others are generated and compared with the same set of four triangle waveforms. Thus different sets of switching signals for different phases of the inverter have been found.

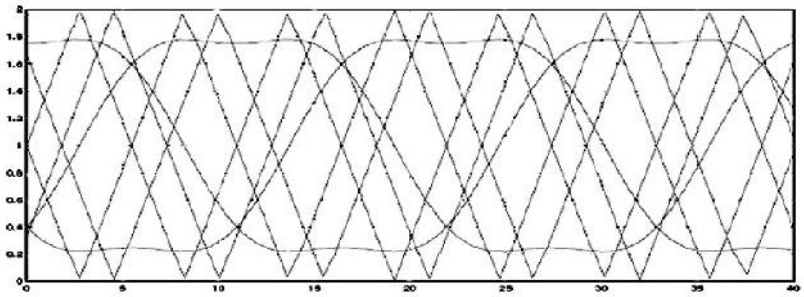

Fig. 5. Carrier and control signals for generating switching signals of three-phase five-level inverter

IV. Simulation and Results

Two types of simulations are performed. The first one consists of measuring THD of the open-circuit voltages of the five-level inverter which is not given here for the brevity of the paper. After open-circuit analysis, the multilevel inverter is now connected to a three-phase induction motor of a rated power of 40HP, a rated speed of 1725 rpm and a rated voltage of 220V (RMS line-to-line voltage at a frequency of 60Hz). No additional physical load is placed at the shaft of the motor.

Fig. 6 and Fig. 7 show the stator and rotor currents of the motor. It is evident from the figure that the currents fluctuate up to 0.65 sec and after that it achieves a constant value. This is because the motor takes about 0.65 sec to reach its full speed of 1725 rpm.

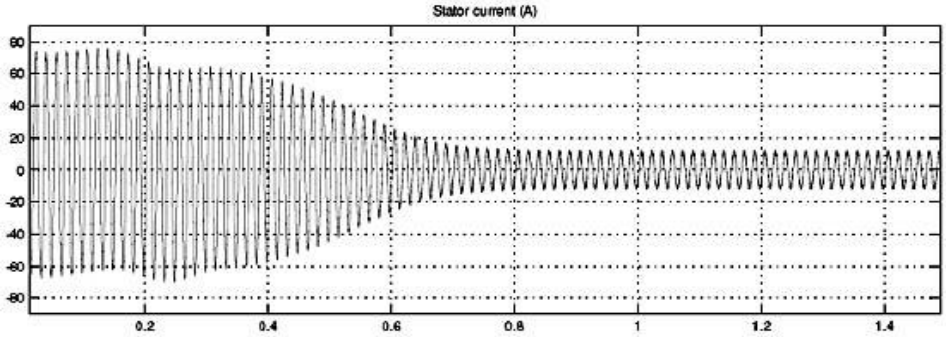

Fig. 6. Stator current I_{sa} of motor

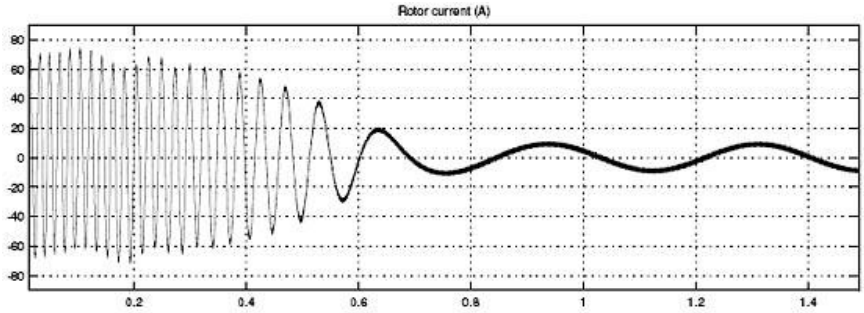

Fig. 7. Rotor current I_{ra} of motor

The extremely high value of current at the starting points of the simulation is due to the fact that before the rotor gains any type of momentum or speed, the stator acts as a very high power load. The fluctuations in the stator and rotor current values die out at about 0.65 sec and the currents achieve a fairly constant value.

Fig. 8 describes the electromagnetic torque characteristic of the motor fed by three phase five-level PWM inverter. At the starting instant the torque has oscillating characteristic. A nearly constant electromagnetic torque is obtained after a time of 0.65 sec.

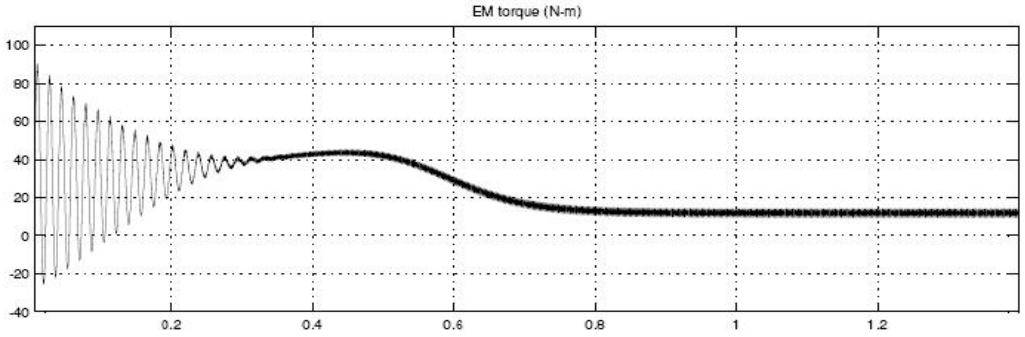

Fig. 8. Electromagnetic torque T_e of the motor

It has been observed that as the stator currents settles to a constant value the electromagnetic torque also achieves a fairly constant value. A zoom in observation of the torque in the steady state reveals that the torque achieves a mean value of about 12 N-m at 0.8 sec.

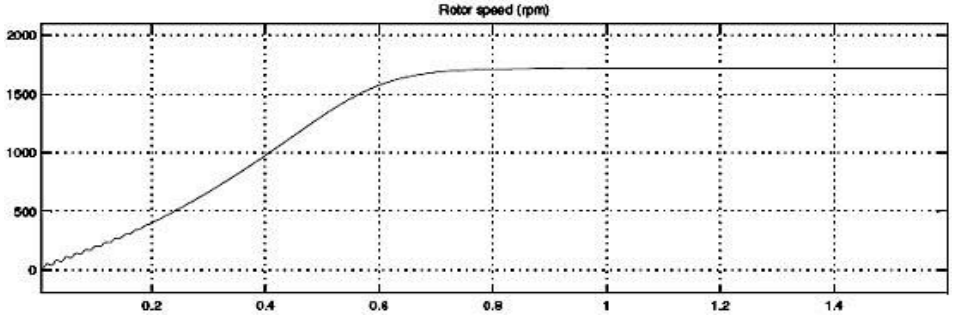

Fig. 9. Speed characteristic of the motor

The speed curve of Fig. 9 shows that the motor is started from stall and very quickly reaches to its speed of about 1725 rpm at 0.65 sec. The speed then settles down to a fairly constant value at its rated speed.

Observation also shows that the rotor and stator currents are quite noisy. The noise introduced by the PWM inverter is also observed in the electromagnetic torque waveform T_e. However the motor's inertia prevents this noise from appearing in the motor's speed waveform.

V. Conclusion

All the simulations have been done with an LC filter at the output of the inverter to minimize the THD at only 5.8%. Also the modulation depth of the inverter is increased to 1.15 by inserting third harmonics to the control signals. This allowed using higher modulation index which gave minimum harmonic distortions. The designed inverter has been tested with an asynchronous induction motor of rated power 40HP and 220V. Investigations show that the motor started from the stall and reaches to its optimum speed within 0.65 sec. Also the inverter introduces some noise to rotor and stator currents as well as to the electromagnetic torque waveform. But this does not affect much to motor's speed due to inertia. Also the leakage inductance of the induction motor and the inertia of the mechanical system act as a filter for current harmonics. Hence the THD for current waveform gives a satisfactory result when induction motor has been used.

---

1. Peng F. Z., J. S. Lai, 1996, "Multilevel Converters – A New Breed of Power Converters", IEEE Transactions on Industry Applications, **32**, 3, 509-517.
2. Nabae A., I. Takahashi, H. Agaki, 1981, "A New Neutral-Point-Clamped PWM Inverter", IEEE Transactions on Indus`1try Applicaitions, IA-17, **5**, 518-523.
3. Bhagwat P. M., V. R. Stefanovic, 1983, "Generalized Structure of a Multilevel PWM Inverter", IEEE Transactions on Industry Applications, **IA-19**, **6**, 1057-1069.
4. Walker G. R., 1999, "Modulation and Control of Multilevel Converters", Ph.D. thesis, University of Queensland 4072.
5. Meynard T., H. Foch, 1992, "Multi-level Conversion: High Voltage Choppers and Voltage Source Inverters", IEEE PESC'92, 397–403.
6. Meynard T, H. Foch, 1993, "Imbricated Cells Multi-level Voltage Source Inverters for High Voltage Applications", European Power Electronics Journal, **3(2)**, 99–106.
7. Krause P. C., O. Wasynczuk, S. D. Sudhoff, 2002 "Analysis of Electric Machinery and Drive Systems", IEEE Press.
8. Corzine K., 2005, "Operation and Design of Multilevel Inverters", Developed for the Office of Naval Research, USA.